Scientific Research Publishing

Journal of Water Resource and Protection, 2023, 15, 557-580
https://www.scirp.org/journal/jwarp
ISSN Online: 1945-3108
ISSN Print: 1945-3094

Standardized Baseflow Drought Index Comparison to SPEI in High Baseflow Streams

Katherine A. Clancy

College of Natural Resources, University of Wisconsin at Stevens Point, Stevens Point, USA
Email: kclancy@uwsp.edu

How to cite this paper: Clancy, K.A. (2023) Standardized Baseflow Drought Index Comparison to SPEI in High Baseflow Streams. *Journal of Water Resource and Protection*, **15**, 557-580.
https://doi.org/10.4236/jwarp.2023.1511031

Received: August 11, 2023
Accepted: November 6, 2023
Published: November 9, 2023

Abstract

Increased use of streamflow, most importantly minimum flow/baseflow data should be incorporated into drought indices, especially in regions where streams have a high baseflow component. Standard departure for streamflow (SDSF) and standard departure for baseflow (SDBF) were compared to the standardized precipitation and evapotranspiration index (SPEI) drought index values for 17 baseflow-dominated watersheds in the northern, central, and southern regions of Wisconsin. For each watershed, comparisons of SDSF, SDBF, and SPEI time series (for 1, 3, and 12-month time scales) were evaluated using correlation, run lengths of negative and positive values, sign congruence, and Mann-Kendall trend test. In general, SDBF performed better than SDSF for longer time scales. Trends of wetness appear to be distinguished earlier in SDBF compared to SDSF and SPEI-1, SPEI-3, and SPEI-12. The results of this study are consistent with regional statewide climate studies on precipitation and changes in precipitation intensity. This study highlights how standardized baseflow data are robust and compare to SPEI 12-month time scales.

Keywords

SPEI, Baseflow, Drought Indices, Streamflow

1. Introduction

Drought is often considered one of the most complex natural disasters to identify. Drought conditions are often detected only during long spates of precipitation deficiencies [1] [2] [3] [4] [5]. Streamflow and groundwater are subject to meteorological cycles and direct human impacts through diversions such as pumping for agricultural and drinking water. Streamflow and groundwater levels are also affected by indirect human impacts such as land cover changes and vegetative changes. Decreased streamflow and groundwater levels may reveal

early signs of human-induced drought before precipitation deficiencies occur, but the complex nature of hydrology phenomena and seasonal vegetation cycles can give conflicting information, especially about the severity of drought [1] [3] [5] [6] [7].

The study of climatic patterns has contributed to different categories of drought including meteorological drought (precipitation deficiencies), hydrologic drought (streamflow and groundwater deficiencies), agricultural drought (typically associated with soil water moisture deficiencies), and economic drought (impacts from multiple forms of drought that impact the economy) [7] [8]. Our evolving understanding has resulted in a significant increase in the number of drought indices that are used to detect moisture conditions in a variety of ways [2] [5] [9] [10].

The World Meteorological Organization [3] publishes a compendium that includes 50 of the most widely used indices. WMO organizes them by the "ease-of-use" and data requirements with the following categories: green (easy to use and daily data are not required), yellow (moderately easy but may require multiple variables and proprietary code), and red (difficult to use due to complexity of calculation and data requirements). Most of the indices rely upon precipitation and temperature data. Streamflow data represents 10% of the drought indices published in the WMO (two in the yellow and three in the red index ease of use categories). While the WMO list is not exhaustive, it does represent the dominant indices commonly used as the most common variables and data used to evaluate drought [3].

The omission of streamflow from most drought indices is not due to a lack of observed data, especially in the United States and Canada. The United States Geological Survey has over 82,000 streamflow gages with more than 60% having over 30 years of data [11] [12]. Regardless, streamflow is not included in many indices because of its complexity. Streamflow is a mixture of direct precipitation, surface runoff, and groundwater. Each component has a different time of concentration, and the lags associated with groundwater contributions can be especially confounding. Streamflow is also affected by basin size, the connectivity to aquifers, and watershed land and soil cover [11].

Despite the challenges, there are several advantages of including streamflow in drought indices. The flow component of streamflow provides an integrated representation of recent precipitation and temperature. The baseflow component of streamflow yields information about groundwater over longer time scales. Streamflow gives a better representation of available water at a local scale. Finally, streamflow is a tangible variable that the public can easily visualize.

Understanding widely used meteorological drought indices is instructive in the development of a streamflow index. Precipitation and temperature data are used extensively in drought evaluation they are independent of basin size. To further enhance interpretation, precipitation and temperature are standardized and incorporated into spatial models such as the standardized precipitation

index (SPI) [13] and the standardized precipitation and evaporation index (SPEI) (Vicente-Serrano *et al.*, 2010) [14] [15]. SPEI is a relatively new drought index [14] [15] [16]. Like SPI, SPEI is used to evaluate and characterize meteorological droughts. SPEI uses multiple precipitation gauges with over fifty years of data to develop regional SPI values at different time scales. It provides spatial and temporal information about how precipitation differs from the baseline period. Time scales such as one month correspond well with average month precipitation. One-to-three-month SPI and SPEI time scales have been demonstrated to correspond well with surface water levels, and longer time scales (greater than six months) are expected to correspond well with groundwater [17].

A significant limitation of SPI as a drought index is the obvious absence of temperature or evapotranspiration (ET) impacts. SPEI attempts to remedy this omission by including ET models in the SPI. In simplest terms, the SPEI is developed by using the SPI values for a region and subtracting the ET values. ET values are calculated using the location's latitude and an ET model (Thornthwaite or Hargreaves are commonly used), which only requires monthly temperature data. The standardized values are fit using a lognormal distribution, which reduces the complexity and accounts for the growing acceptance of SPEI [14] [15] [16].

SPI uses a gamma probability distribution rather than more commonly used distributions such as the lognormal or log-logistic distribution [13] [14] [15] [16] [18]. Standardization of streamflow data reduces its dependence on basin size and allows for flow data to be comparable across basins. Some of the earliest standardized streamflow indices (SSIs) were developed by fitting monthly streamflow data to probability distributions including the gamma distribution and Weibull distributions as well as other less common distributions. The method was improved upon by Vicente-Serrano *et al.* (2012) [19], who also developed the SPEI. After testing multiple distributions, Vincente-Serrano *et al.* (2012) [19] found that the SSI could best be developed using a monthly best-fit and minimum orthogonal distance. Their investigations found that each watershed needed to be calibrated to determine the best distribution for its flow data.

The research described in this paper builds upon Vincente-Serrano *et al.* (2012) [19] by comparing the baseflow component of streamflow to SPEI time scales. The addition of baseflow is expected to give greater insight into longer-term wet and dry patterns. Baseflow is highly correlated with groundwater levels in regions that have high baseflow indices (BFIs) and may give a more integrated view of meteorological impacts to a region [17]. Land use, basin size, latitude, and the length of the streamflow record are also investigated for their overall impact on SDBF and SDSF in comparison to other watersheds within the study. Baseflow may prove to be a tool to gain insight into groundwater recharge and levels, which are often challenging to characterize due to limited data.

2. Study Area

Wisconsin has high baseflow contributions to many of its streams [20]. The two main criteria for the study watershed selection were length on continuous discharge record that was greater than 10 years and a high baseflow component. Our third criterion was to find a range of watershed sizes. Our selection yielded seventeen gauged watersheds as shown in Figure 1. The baseflow index was computed for each watershed. The baseflow index is the ratio of the baseflow component to the total flow.

The watersheds ranged in size from 2.17×10^7 m^2 to 1.58×10^9 m^2 with an average size of 5.05×10^8 m^2. The average baseflow component of the watersheds was 74 percent. Station summary data are in Table 1.

Watersheds were categorized by their size (large: 1.6×10^9 to 5.6×10^8 m^2; medium: 5.2×10^8 to 3.2×10^8 m^2; small: 2.1×10^8 to 2.2×10^7 m^2) as well as their latitude in the state (Northern: above 45.2˚, Central: between 44.3˚ and 43.5˚, and Southern: below 43˚) (Table 2). The relative size and location of the watersheds can be seen in Figure 1, and this information is summarized in Table 2.

Table 1. Watershed site information, including USGS station ID, full USGS station name, and the short name used in this paper. The end and beginning of continuous record (except for Baraboo which is missing 10 years of data). The location description was determined for the purposes of this research.

Station ID	USGS Station Name	Short Name	Record Start	Record End	Location
5357215	Allequash Creek at Cty Hwy M Nr Boulder Junction	Allequash	1991	2023	north
5405000	Baraboo River Near Baraboo	Baraboo	1942	2023	central
5357335	Bear River Near Manitowish Waters	Bear	1991	2023	north
5431486	Little Turtle Crk at Carvers Rock Rd N Clinton	Clinton	1939	2023	south
4026349	North Fish Creek Near Moquah	Fish	1989	2015	north
5543830	Fox River at Waukesha	Fox	1963	2023	south
5413500	Grant River at Burton	Grant	1934	2023	south
5408000	Kickapoo River at La Farge	Kickapoo	1938	2023	central
4087120	Menomonee River at Wauwatosa	Menomonee	1961	2023	south
5414000	Platte River Near Rockville	Platte	1934	2023	south
5394500	Prairie River Near Merrill	Prairie	1914	2023	north
5432500	Pecatonica River at Darlington	Pecatonica	1939	2023	south
5382325	La Crosse River at Sparta	Sparta	1992	2023	central
5393500	Spirit River at Spirit Falls	Spirit	1942	2023	north
4027500	White River Near Ashland	White	1948	2023	north
5429500	Yahara River at Mc Farland	Yahara	1930	2023	south
5402000	Yellow River at Babcock	Yellow	1997	2023	central

Table 2. Descriptive information for the study watersheds. The size category was determined for the purposes of this research.

Watershed Name	Agricultural	Wetland	Forest	Urban	BFI %	Area (m^2)	Size Category
Allequash	0.82	16.88	56.2	4.34	90	2.18E+07	small
Baraboo	59.02	2.03	31.06	6.85	71	1.58E+09	large
Bear	0.4	26.92	40.32	5.14	88	2.11E+08	small
Clinton	79.78	0.82	6.69	10.46	77	5.15E+08	medium
Fish	12.64	4.96	67.14	4.20	81	1.69E+08	small
Fox	26.23	7.63	12.24	48.98	70	3.26E+08	medium
Grant	78.76	0.27	14.78	5.99	75	6.97E+08	large
Kickapoo	49.44	0.49	43.49	4.78	78	6.89E+08	large
Menomonee	20.62	5.94	6.87	65.58	52	3.19E+08	medium
Platte	79.99	0.28	14.81	4.77	75	3.68E+08	medium
Prairie	12.42	24.73	55.88	4.82	76	4.77E+08	medium
Pecatonica	85.37	0.28	8.38	5.70	61	7.07E+08	large
Sparta	37.81	3.37	47.71	8.51	89	4.33E+08	medium
Spirit	9.18	17.39	66.4	3.28	58	2.11E+08	small
White	6.54	12.38	67.75	3.70	83	7.80E+08	large
Yahara	50.98	5.09	6.2	28.18	91	7.52E+08	large
Yellow	62.32	2.89	27.48	6.51	47	5.57E+08	large

3. Methods

3.1. Flow Data and Baseflow Separation

The USGS national water database was accessed in April of 2023 to obtain daily flow data [12]. Techniques for separating total streamflow into baseflow and runoff can range from the simple to the complex and subjective, requiring recalibration for each independent storm and watershed. Sloto and Crouse's (1996) [21] publication made use of a simplistic filter that was adopted by the USGS and developed into a computer program, HYSEP. Advances have been made in hydrograph separation since Sloto and Crouse's (1996) work [21] [22] [23] [24]. Certain stable isotopes (primarily ^{2}H and ^{18}O) are very sensitive to changes in the source of water (groundwater, atmospheric, or runoff). In the past decade isotopic analysis has increased insight into the accuracy of well-established methods for hydrograph separation [22] [25] [26]. The limitations of stable isotope separation are significant. Stable isotope analysis is expensive, time intensive, and simply not available on a large scale for multiple sites.

Another advance in baseflow separation is the use of temperature sensors for hydrograph separation [27] [28]. This method was used in a series of studies to improve streamflow separation, especially in watersheds with snowmelt contribution to their stream waters [27] [28]. The knowledge derived from these studies

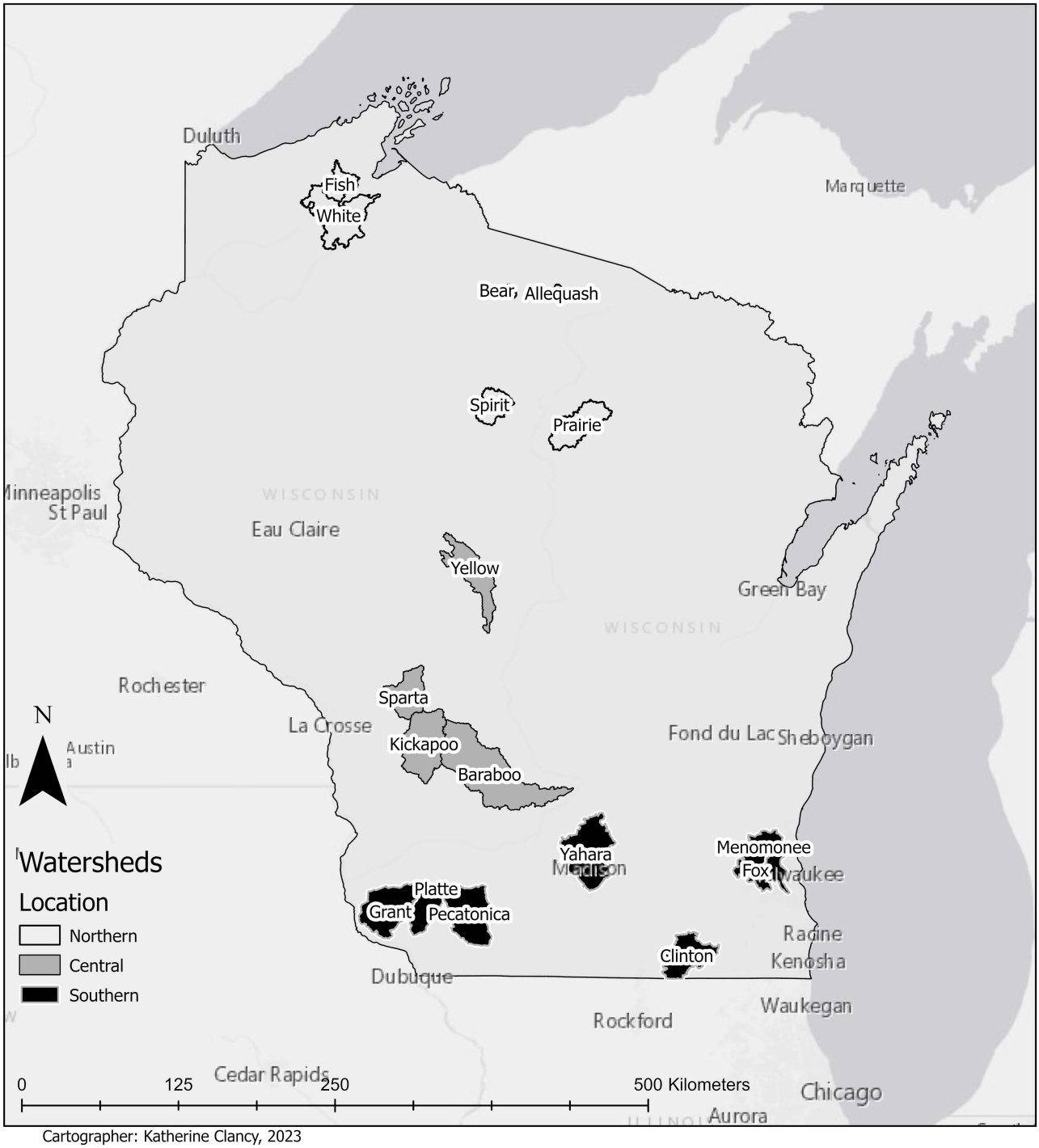

Cartographer: Katherine Clancy, 2023

Esri, HERE, Esri, HERE, Garmin, USGS, EPA, Esri, HERE, NPS, Esri, HERE, Garmin, USGS, EPA, NPS

Figure 1. Watershed map with legend key for designation of the north, central, and southern locations.

has improved the baseflow separation accuracy when the date of spring melt is known. Like isotopic separation, the method requires a substantial investment in equipment and labor. It is worthy of investigation and a study of its own, but these types of advances are beyond the scope of this paper and beyond the means of most research investigations.

For the reasons mentioned, the HYSEP program was used to separate the data into daily flow and runoff [21]. Despite HYSEP's age, it is currently used extensively by USGS and has been cited by over 800 papers. The HYSEP developers tested several methods: fixed interval, sliding-interval, and local-minimum methods. For our purposes, the local minimum average (using three points) is the best method to use for flow separation especially when aquifer porosity is unknown and would have to be inferred. The HYSEP program separates total flow into runoff and baseflow. Using this program, throughflow or interflow is most likely to be categorized as baseflow, while direct precipitation is probably categorized as direct runoff. For the goals and requirements of this research, this simplified division of total flow is acceptable.

3.2. Watershed Delineation and Landcover

The study region's seventeen watersheds were delineated using the *D8 method* of watershed delineation that is a part of ESRI's ArcGIS Pro (ver. 3.1) Hydrology Tools. This method is one of the most used methods of watershed delineation and is outlined in Troolin and Clancy (2016) [29] and based on the work of Jenson (1984) [30]. The method only requires the input of elevation data (*i.e.* digital elevation models) and an outlet. The 30-meter digital elevation model from USGS was used [31]. The area and perimeter of the watersheds were compared to the values published on the USGS website and were found to be within 99 percent of the area. Landcover was obtained from the USGS at a 30-meter resolution [32].

3.3. SPEI

SPEI data are available in the public domain in a spatial-time format called netcdf [17]. Netcdf files are layers of gridded spatial (raster) data. Each raster (gridded layer) represents a slice of time. For SPEI the resolution is approximately monthly. Monthly data for SPEI is available in Wisconsin from 1901-2021 at a resolution of 0.5 degrees. Values can also be determined using R code that is described in Vicente-Serrano (2010) [14].

SPEI values for the study watersheds were obtained [17]. Some watersheds extended across multiple grids. For these watersheds, the monthly SPEI values for 1901-2021 were available for each watershed for 1, 3-, 12-, 18-, and 24-month time scales. SPEI monthly values were available for 6 and 9 months from 1901-2015.

SPEI annual values were determined from the monthly SPEI gridded values for each watershed. The values are standardized values, so it was unnecessary to further standardize the values. Seven SPEI times scales were examined: 1 month (SPEI-1), 3 month (SPEI-3), 6 month (SPEI-6), 9 month (SPEI-9), 12 month (SPEI-12), 18 month (SPEI-18), and 24 month (SPEI-24). Based on the data evaluation, SPEI-6 and SPEI-9 were excluded because they only have values from 1901 to 2015, while the other SPEI data have values from 1901-2021. SPEI-6 and

SPEI-9 were not significantly different from the SPEI-3. SPEI-18 and SPEI-24 were also excluded because the values and patterns were not significantly different. This reduced the study to SPEI-1, SPEI-3, and SPEI-12 for each watershed. SPEI monthly data were converted to annual data for 1901-2021 by using the average annual value for each watershed.

3.4. Statistics

The statistical calculations described in this paper were performed in Rstudio (2023.03.01) using R (version 4.3.0). Monthly, seasonal, and annual values were determined from daily flow, baseflow, and runoff values for each watershed. BFI was also calculated using daily data.

Stream data were log transformed based on Vincente-Serrano *et al.* (2012) [19]. The minimum, maximum, average, sum, and cumulative sum were determined for annual, seasonal, and monthly data. The annual average was calculated using the log transformed values of flow data to develop the standard departure for baseflow (SDBF) and standard departure for streamflow (SDSF).

To compute a comparative flow index, all flow data were standardized [13] [15] [19]. Standardized data allows for better comparison across watershed size, and it is easier to see trends within the time series. The annual standard departure for streamflow (SDSF) and standard departure for baseflow (SDBF) were developed by collapsing daily data into annual data by using the annual mean. The mean and standard deviation were calculated for the annual data set and used to develop the standard departure for each watershed's flow data. The formula for determining SDSF and SDBF is shown in Equation (1).

$$SD = \frac{\left(X_i - \mu\right)}{\sigma} \tag{1}$$

In Equation (1), SD is the standard departure for the dataset (either SDSF or SDBF) and x_i represents the log of the annual flow value for one year within the dataset, μ represents the average of the entire log of the annual dataset, and σ is the standard deviation of the log of the annual dataset.

SPEI data are standardized for the reported time period (1901-2021). Standardization allows comparisons between data types to be more useful and intuitive. The nature of standardized data such as SPEI, SDBF, and SDSF values is that they have negative or positive values. Negative values represent drier conditions and positive values represent wetter conditions relative to the base period of the data.

3.4.1. Correlation

The SDBF, SDSF, and SPEI annual data were evaluated using several metrics. Linear correlation was used to test the relationship between SDBF and SDSF to the different SPEI time scales (1, 3, and 12 months). The expectation is that SDSF would show higher correlation to shorter time SPEI time scales (SPEI-1 and SPEI-3) than SDBF. Alternatively, SDBF would have higher correlation (com-

pared to SDBF correlation values) with SPEI-12 than SDSF. To obtain the Pearson correlation coefficients (R^2) values the *cor package* in R was used for data matched by year.

3.4.2. Mann-Kendall Trend Test

The overall trend of the SDBF, SDSF, and SPEI time scales [1] [3] and [12] data were evaluated using the Mann-Kendall tau trend test using the *Kendall* R package. The Mann-Kendall is a non-parametric statistical hypothesis test using the rank of the data to detect trends [33] [34]. It is a commonly used hypothesis test in hydrologic time series data, especially gaining acceptance with the inclusion of a statistical manual for hydrologists [35] and due to its flexibility in examining stationarity in a wide range of climate variables [36] [37] [38].

For the Mann-Kendall hypothesis test, the null hypothesis (H_0) assumes the data are random (there is no trend), and the alternative hypothesis is there is a trend (up or down). Using an alpha of 0.05, all p-values less than 0.05 were assumed to have a trend. The direction of the trend is generally determined by examining the data graphically. Limitations to the Mann-Kendall tau trend test include an assumption that the data only have a monotonic trend, which means that the data can only have one trend [35]. Data with multiple trends will often indicate that there is "no trend." Generally, data sets with complex trends that include both up and down trends should be divided into subsets and analyzed separately. The examination of the data and comparison of similar trend results (*i.e.* "no trend" or "trend") among a watershed's datasets (SDBF, SDSF, and SPEI-1, SPEI-3, and SPEI-12) was the main purpose of the Mann-Kendall test.

3.4.3. Time Series Patterns: Run Length and Sign Concordance

A common analysis to characterize the persistence of a drought is time-series run theory [17] [39] [40]. Run theory calculates the number of sequential occurrences of a particular value (negative or positive) and may include a magnitude threshold. For this study, a magnitude threshold was not used. Data were considered either positive or negative. R script was written to determine maximum negative and positive run length in SDBF, SDSF, and SPEI [1] [3] and [12] data for all watersheds. The year of the maximum run length was also recorded for each watershed's datasets. This allows for determining how well the data match within each watershed as well as patterns across the watersheds.

A follow up analysis to the run length was to evaluate the sign concordance within the dataset. While not as common an analysis as run length, sign concordance can help evaluate large scale patterns [41]. Evaluation of concordant pairs within time series compares the signs of the values for the same time within the datasets. In this analysis, concordant pairs are data that have the same sign for a year. The absolute value of concordant pairs and the percentage of concordant pairs were recorded using an R script written by the author for this study. Sign concordance was determined by comparing SDBF to SPEI-1, SPEI-3, and SPEI-12 as well as SDSF to SPEI-1, SPEI-3, and SPEI-12.

4. Results

4.1. Correlation

The correlation coefficient values between SPEI time scales and SDSF and SDBF are summarized in Table 3. The flow variables maximum R^2 value and associated SPEI-1, SPEI-3, and SPEI-12 scale are reported. The R^2 range for SDSF is 0.44 - 0.73. Three of the four watersheds with R^2 values below 0.50 are northern watersheds. Northern watersheds, Bear and Allequash, have values 0.64 and 0.69, respectively. The SPEI time scale that best agreed to SDSF was the SPEI-3 (11 out of 17 watersheds). Bear, Grant, and Allequash watersheds (all Northern watersheds) had the highest correlation with SPEI-12 data. Prairie, Fish, and Menomonee had the highest correlation with 1-month SPEI data.

The range for R^2 values of SDBF and SPEI-12 months was wider than the SDSF range, with values from 0.35 - 0.78. Among the six watersheds with R^2 values below 0.50, four were northern watersheds: Fish, Prairie, White, and Spirit. Roughly half of the watersheds' SDBF data reported the highest correlation with SPEI-12, while the other half were SPEI-3. None of the watersheds had their highest correlation with SPEI 1-month data for SDBF.

Table 3. This table contains the results of the Mann-Kendall trend results. The watershed location is duplicated (from Table 2) to aid in the convenience of determining trend patterns by latitude. The max correlation result is reported along with the scale. The max SDSF R^2 correlated best with SPEI-3, while max SDBF R^2 correlated best with SPEI-12.

Watershed Name	Location	SDSF Trend	SBFI Trend	SPEI	Max R^2, SDSF	SPEI Scale (SDSF)	Max R^2, SDBF	SPEI Scale (SDBF)
Allequash	north	NS	NS	NS	0.69	12	0.70	12
Baraboo	central	up	up	up	0.57	3	0.57	12
Bear	north	NS	NS	NS	0.64	12	0.67	12
Clinton	south	up	up	up	0.67	3	0.70	12
Fish	north	NS	NS	NS	0.48	1	0.35	3
Fox	south	up	up	up	0.64	3	0.61	3
Grant	south	up	up	up	0.69	12	0.70	12
Kickapoo	central	up	up	up	0.61	3	0.65	12
Menomonee	south	up	up	up	0.68	1	0.78	3
Pecatonica	south	up	up	up	0.48	3	0.44	3
Platte	south	up	up	up	0.61	3	0.72	12
Prairie	north	NS	NS	up	0.47	1	0.43	12
Sparta	central	up	up	NS	0.62	3	0.63	12
Spirit	north	up	up	up	0.49	3	0.49	3
White	north	NS	NS	up	0.44	3	0.46	3
Yahara	south	up	up	up	0.73	3	0.72	3
Yellow	central	up	up	up	0.51	3	0.45	3

4.2. Sign Congruence

On average the sign congruence between SPEI and the flow variables (SDBF and SDSF) was approximately 73 percent for the entire data set, as summarized in Table 4. The congruence percentage increased with increasing time scale. Values calculated were 70, 73, and 76 for the SDBF and SPEI 1, 3, and 12 month, respectively. The congruence percentages for SDSF showed a similar pattern to SDBF where values were 71, 74, and 76.

Similar to the correlation results, the highest sign congruence was between SDBF and SPEI-12, with percent agreement ranging from 52 - 91. SDSF highest sign congruence was with SPEI-3, but the percent value of 73 was only marginally higher than SPEI-1 and SPEI-12 (averaging 71 percent). Results from northern watersheds did not stand apart from the other watersheds.

4.3. SPEI Mann-Kendall Trend Results of the Data

The Mann-Kendall trend test results for a monotonic trend are shown in Table 3

Table 4. This table summarizes the results of the percentage of sign congruence between the SPEI time scales. The bold values represent the flow data (SDBF or SDSF), which had the highest sign congruence. For SPEI-1 and SPEI-3, SDSF has slightly higher sign congruence. For SPEI-12, SDBF has significantly higher sign congruence.

Watershed Name	*SPEI-1*		*SPEI-3*		*SPEI-12*	
	SDBF	SDSF	SDBF	SDSF	SDBF	SDSF
Allequash	70	67	70	67	70	67
Baraboo	66	67	69	70	72	67
Bear	80	83	80	83	80	83
Clinton	74	77	79	82	80	77
Fish	68	68	74	84	74	68
Fox	86	84	84	79	91	84
Grant	66	69	70	74	80	69
Kickapoo	63	64	69	70	73	64
Menomonee	75	78	80	80	75	78
Platte	67	68	70	71	71	68
Prairie	72	70	75	77	83	70
Pecatonica	74	70	74	72	77	70
Sparta	52	52	48	56	52	52
Spirit	76	76	84	84	86	76
White	64	64	64	62	81	64
Yahara	74	74	74	71	82	74
Yellow	68	70	75	75	75	70
Average	**70**	**71**	**73**	**73**	**76**	**71**

and indicate that the SPEI data show an upward trend for the 1, 3, and 12 month SPEI data with a few notable exceptions. The northern watershed results are not consistent. From Map 1, Prairie and Spirit are the most southern of the northern watersheds. Their SPEI trends are similar to the central and southern watersheds with a significantly upwards trend. Fish, the most northern watershed, has SPEI data with no significant trend. Allequash and Bear only had significantly upward trends with SPEI-12 data. The most unexpected results are of White watershed. White watershed is just slightly south of Fish watershed, but unlike Fish the SPEI data have a significantly upward trend across all the SPEI time scales.

SPEI for northern watersheds was less likely to show a trend. In Figure 2, SPEI-1, SPEI-3, and SPEI-12 for Prairie watershed (northern watershed) show that especially after 1975 the conditions switch between wet and dry alternating approximately every 3 - 5 years.

In contrast to Figure 2, Figure 3 shows a representative time series of SPEI-1, SPEI-3, and SPEI-12 for central and southern watersheds. Note that after 1975,

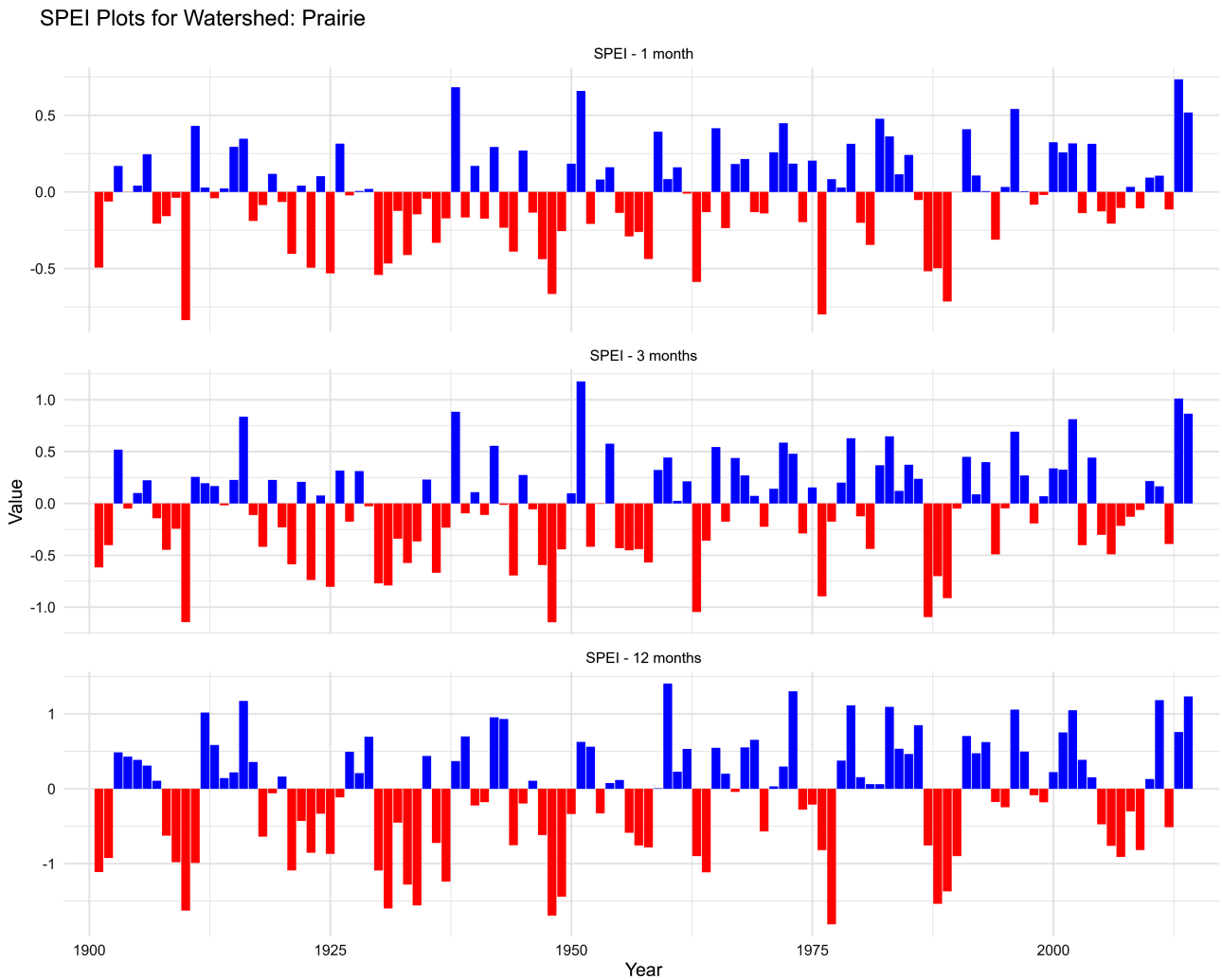

Figure 2. The data are specific to the Prairie watershed, but gives a graphical example of the wet/dry pattern found in SPEI data in the later period in the Northern watersheds.

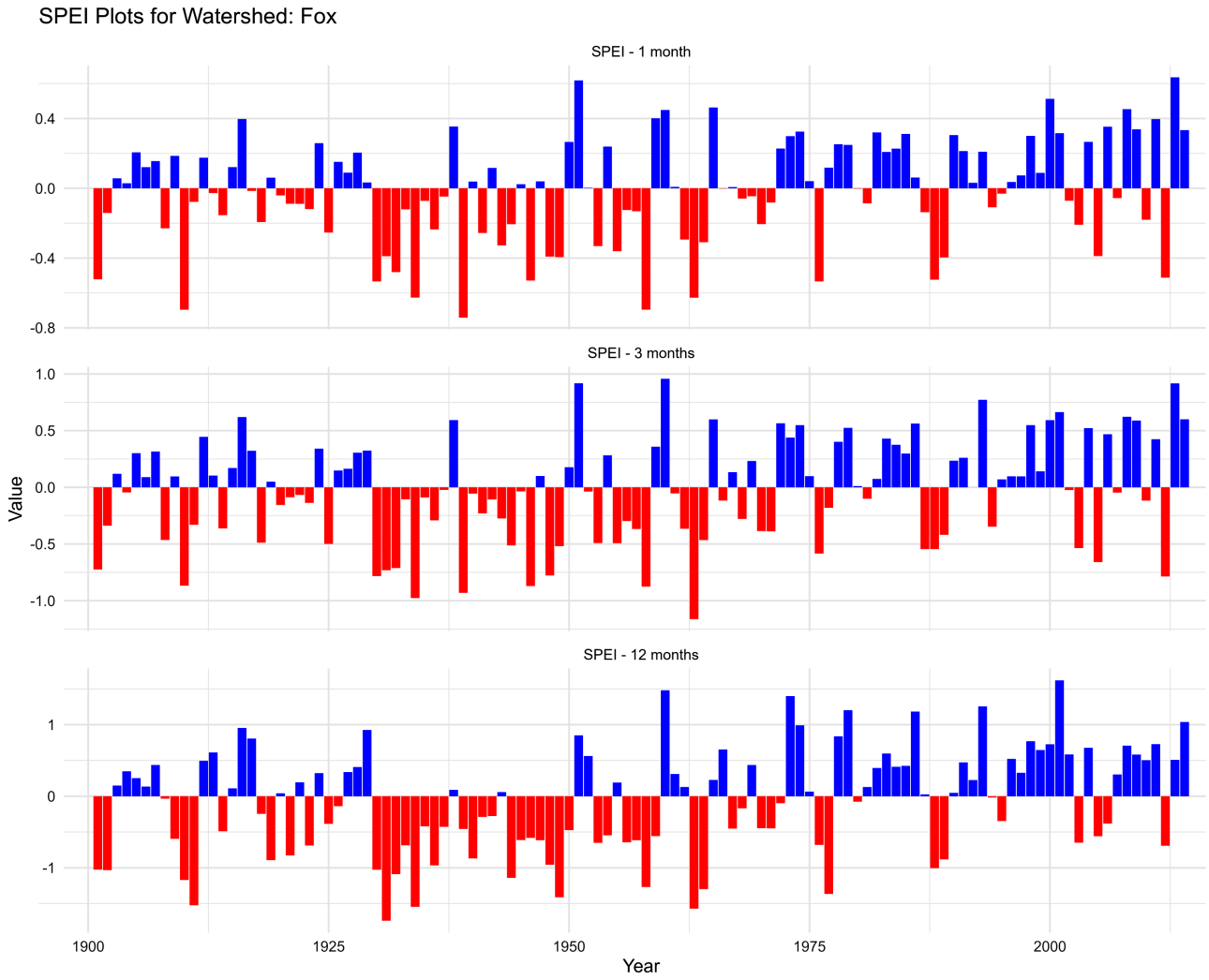

Figure 3. The data are specific to the Fox watershed, but gives a graphical example of the wet pattern found in the SPEI in the later period in the Central and Southern watersheds. The pattern can best be seen in the SPEI-12 data where the number of negative values (shown in red) decreases and the length of the runs is substantially lower than the length of the runs after 1970.

the majority of the values are positive. The trend strengthens as the time scale increases from 1 month (SPEI-1) to 12 month (SPEI-12) time scale.

4.4. Flow Mann-Kendall Trend Results

The Mann-Kendall trend test results for a monotonic trend are in **Table 3** and generally show agreement between annual SDBF and SDSF for the watersheds. Like the SPEI trend analysis, the SDBF and SDSF do not have significant trends for the northern watersheds (Allequash, Bear, Fish, Prairie, White). Spirit watershed is the only northern watershed that differs in pattern. Spirit's SDSF has a significantly positive trend, and the SDBF shows no significant trend.

Figure 4 shows a representative northern watershed pattern using Prairie as an example. The negative or dry periods (red) are as long with similar magnitude as the wetter periods (blue). Compare this image to **Figure 5**, which shows SDBF and SDSF patterns representative of central and southern watersheds. In

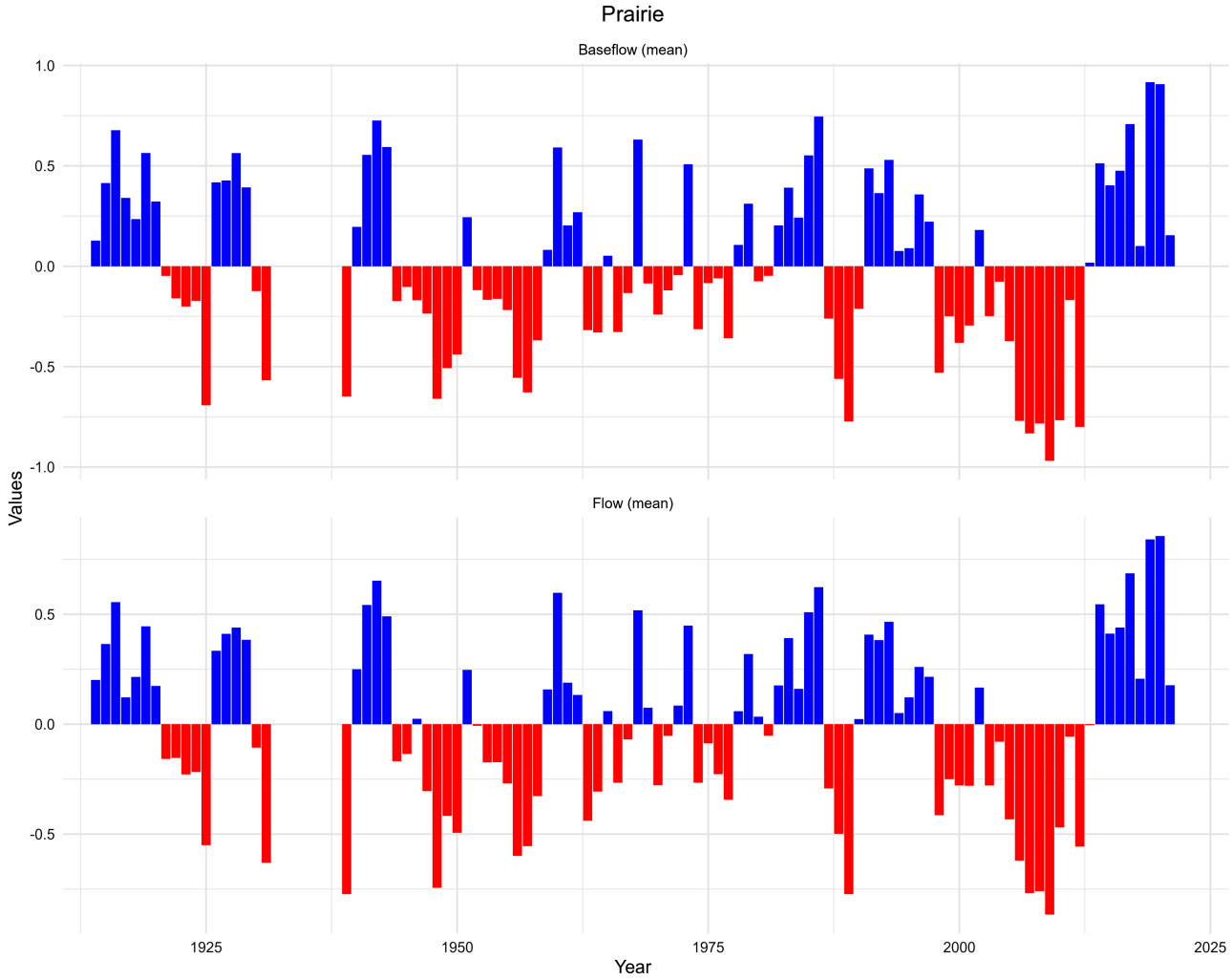

Figure 4. This figure shows the Prairie watershed flow data. This graph shows an example of the wet/dry pattern found in flow data in the later period in the Northern watersheds.

most of the central and southern watersheds SDSF values after 1975 tend to be mostly positive. Also note that SDBF has more positive values of slightly higher magnitude than SDSF.

4.5. SPEI Data Run Pattern

The SPEI run pattern results in **Table 5(a)** corroborate the trend result data but also add additional information associated with SPEI times. All watersheds have longer max positive runs lengths than negative ones. Maximum positive runs appear later in the times series. The start year for positive max runs are 2012, 2005, and 2002, for SPEI-1, SPEI-3, and SPEI-12, respectively. Also of note is that the max positive run length occurs earlier as SPEI time scales increase from SPEI-1 to SPEI-12 suggestive of identifying a pattern of wetter conditions.

Max negative run lengths do not have as consistent a pattern as the positive values. In particular, max run lengths are three years shorter on average. The timing of the max negative run length has a very wide range compared to the

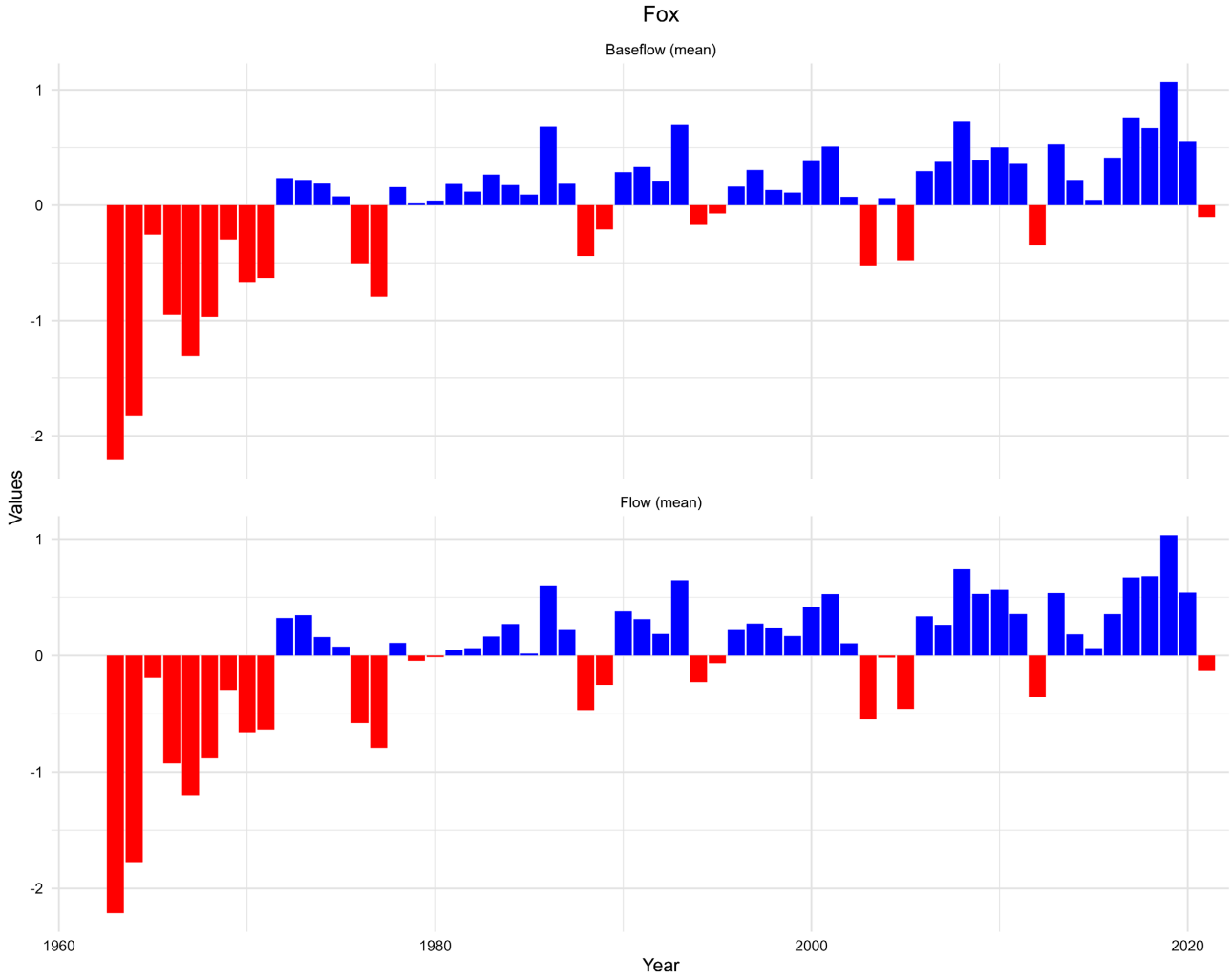

Figure 5. The data are specific to show the Fox watershed flow data. This graph gives an example of the increasing wet pattern found in flow data in the later period in the Central and Southern watersheds.

Table 5. (a) This table summarizes the run length associated with the SPEI data's sign. Negative run length data are in parenthesis. Of note is that the negative run length is long and has an earlier start year, similar to the flow data pattern; (b) This table summarizes the run length associated with the flow data's sign. Of note is that the negative run length is longer and has an earlier start year.

(a)

	Positive (*Negative*)					
Watershed Name	**SPEI-1**	**SPEI-3**	**SPEI-12**	**SPEI-1, Year**	**SPEI-3, Year**	**SPEI-12, Year**
Allequash	8 (8)	8 (5)	8 (7)	2013 (2005)	2013 (2005)	2013 (2004)
Baraboo	8 (4)	7 (4)	8 (7)	2013 (1955)	1996 (1955)	2013 (1953)
Bear	8 (8)	8 (5)	8 (7)	2013 (2005)	2013 (2005)	2013 (2004)
Clinton	8 (4)	7 (8)	13 (7)	2013 (1943)	1995 (1939)	1990 (1944)
Fish	3 (2)	9 (5)	7 (6)	2000 (1989)	1990 (2006)	1996 (2005
Fox	8 (4)	7 (3)	8 (3)	2013 (1968)	1995 (1987)	2013 (1970)

Continued

Grant	8 (7)	8 (7)	12 (6)	2013 (1952)	2013 (1952)	1991 (1953)
Kickapoo	8 (4)	8 (4)	8 (7)	2013 (1946)	2013 (1955)	2013 (1953)
Menomonee	8 (4)	7 (3)	8 (7)	2013 (1968)	1995 (1962)	2013 (1970)
Pecatonica	8 (5)	8 (4)	12 (6)	2013 (1952)	1995 (1955)	1991 (1953)
Platte	8 (7)	8 (7)	12 (6)	2013 (1952)	2013 (1952)	1991 (1953)
Prairie	8 (5)	8 (5)	9 (6)	2013 (1986)	2013 (2005)	1978 (1921)
Sparta	8 (2)	8 (2)	8 (1)	2013 (1994)	2013 (1994)	2013 (1995)
Spirit	8 (4)	8 (5)	9 (7)	2013 (1946)	2013 (2005)	1978 (2004)
White	8 (8)	8 (7)	8 (7)	2013 (1956)	2013 (1955)	2013 (2004)
Yahara	8 (8)	8 (7)	8 (8)	2013 (1930)	2013 (1946)	2013 (1930)
Yellow	8 (4)	7 (4)	9 (4)	2013 (1946)	1996 (1946)	1996 (1947)
Average	**8 (5)**	**8 (5)**	**9 (6)**	**2012 (1964)**	**2005 (1972)**	**2002 (1968)**

(b)

Watershed Name	*Positive* (*Negative*)		SDBF, Year	SDSF, Year
	SDBF	SDSF		
Allequash	8 (9)	6 (9)	2014 (2005)	2016 (2005)
Baraboo	15 (30)	15 (19)	2007 (1942)	2007 (1953)
Bear	9 (10)	9 (10)	2013 (2003)	2013 (2003)
Clinton	10 (12)	8 (12)	1978 (1939)	2013 (1939)
Fish	2 (5)	2 (5)	1990 (2003)	1990 (2006)
Fox	10 (9)	8 (9)	1978 (1963)	2013 (1963)
Grant	8 (9)	8 (9)	2007 (1934)	2007 (1943)
Kickapoo	14 (25)	14 (12)	2008 (1948)	2008 (1948)
Menomonee	8 (11)	7 (11)	1980 (1961)	1981 (1961)
Pecatonica	9 (7)	9 (7)	1978 (2003)	1978 (2003)
Platte	7 (9)	6 (8)	1981 (1934)	2016 (1934)
Prairie	9 (10)	8 (11)	2013 (2003)	1990 (2003)
Sparta	6 (10)	6 (13)	2016 (1996)	2016 (1995)
Spirit	9 (7)	9 (7)	1978 (2002)	1978 (2003)
White	6 (10)	6 (16)	1951 (2003)	1951 (1997)
Yahara	8 (8)	9 (8)	2013 (1961)	2013 (1961)
Yellow	9 (16)	9 (18)	1978 (1946)	1978 (1947)
Average	**9 (12)**	**8 (11)**	**1993 (1973)**	**1998 (1974)**

positive values. The year range for SPEI-1 is 1946-2005 with an average start year of 1964. Similarly, SPEI-3 max negative run lengths start years range from 1946-2006 and 1930-2005 for SPEI-12.

4.6. Flow Run Pattern

The flow data run pattern results are in Table 5(b). The SDBF and SDSF patterns are similar to one another. Average positive run lengths are nine and eight for the SDBF and SDSF, respectively. Max negative run lengths are considerably longer with an average of 12 (SDBF) and 11 (SDSF), which is different than the SPEI results. The flow results similar to the SPEI data are the timing of the max negative and positive run lengths. The average year of the positive max run length was 1994 (SDBF) and 1998 (SDSF), compared to the average year of the negative max run length of 1971 and 1973 for SDBF and SDSF, respectively.

4.7. Land Use

Watershed land use varied considerably, and it varies on the location within the state. The northern part of the state is mostly forest and wetlands. Agricultural and urban land cover increase progressing south. Northern watersheds have forest ranging from 68 (White) to 40 (Bear) percent. Wetlands make up the second largest category for the study watershed in the north ranging from 27 (Bear) to 5 (Fish) percent. The range in agriculture is 13 (Fish) to 0.4 (Bear) percent. For northern watersheds, the urban percentage is at or below 5 percent. The overall range in the BFI is 90 - 58 percent for northern watersheds.

Central watersheds are mostly forest and agricultural with agricultural land cover ranges from 62 (Yellow) to 38 (Sparta) percent and forest land cover ranges 48 (Sparta) to 27 (Yellow) percent. Wetland land cover values are below five percent for the central region and urban ranges from five (Kickapoo) to nine (Sparta) percent. The BFI percentages for the central region range from 89 to 47 percent. Southern watersheds have the highest amount of urban land cover percentages ranging from 66 (Menomonee) percent to five (Platte). Agriculture is high in the southern watershed with a range of 86 (Pecatonica) to 21 (Menomonee). Wetlands range from eight (Fox) to less than one percent (Platte and Pecatonica). The BFI for this region ranged from 75 to 50 percent.

Land cover percentages or groupings did not show any significant trends as a variable compared across SPEI-1, SPEI-3, and SPEI-12 data. There was no statistically significant difference associated with Mann-Kendall trends, correlation, or sign agreement associated with associated with any of the land use groupings. As described in the run patterns section for both SPEI and flow data, all the northern watersheds exhibited a wet/dry pattern with no monotonic upward trend. Even though northern watersheds have higher amounts of wetland and forest and lower amounts of agriculture and urban areas, there are watersheds within the central region that have similar land cover but do not exhibit the wet/dry period.

4.8. Watershed Size

Watershed size varied within each region. The northern region's average watershed size was 3.12×10^8 sq. m with a range of 1.58×10^9 to 2.18×10^7 sq. m. The central region's average watershed size was 8.14×10^8 sq. m with a range of 7.8×10^8 to 4.33×10^8 sq. m. Finally, the southern region's average watershed size was 5.26×10^8 sq. m with a range of 7.52×10^8 to 3.19×10^8 sq. m. Overall, the northern watersheds were the smallest within the study, and the largest were in the central region.

As a categorical variable, watershed size (large, medium, small) did not show any significant trends as a variable compared across SPEI-1, SPEI-3, and SPEI-12 data. There was no statistically significant difference in Mann-Kendall trends, correlation, or sign agreement associated with associated with any of the land use groupings. The wet/dry pattern was detected in both small and medium size watersheds but not observed in other watersheds in the medium category.

4.9. Length of Record (Data Start and End Dates)

The start and end year of the study varied considerably. The earliest start year (Prairie) was 1914 compared to the latest start year of 1997 (Yellow). Five watersheds had start years after 1988 (Fox, Allequash, Bear, Sparta, and Yellow). When data were standardized to have a start year of 1991 (excluding only Yellow), the monotonic trend test results did not change. Truncated Prairie data (start date shifted from 1914 to 1991) exhibited the wet/dry trend as it did without the shortening of the time series.

Mann-Kendall trend data remained similar with most watersheds reporting an increasing (or wetter) trend with time, but the shift in the wetter period moved from 1990 to 2006-2008. Standardizing the data decreased the average negative run times considerably from 8 to 5 years. Positive run times decreased from eight to seven years, and the start of the run occurred later from the 1990s to the 2006-2009. Correlation and match analysis with SPEI data decreased between 10 - 15 percent. For this reason, the time series available for each stream was used for the data set rather than the truncated data set.

5. Discussion

5.1. Correlation and Congruence

SPEI longer time scales (12 months or greater) are expected to show a higher correlation with groundwater data [14] [15] [16] [17]. It is not unexpected that SDBF data generally have the highest correlation with SPEI-12; however, it is interesting that SPEI-3 (rather than SPEI-1) accounted for the max R^2 within watersheds for SDSF. Seasonal hydrologic impacts may explain why SDBF for certain watersheds do not correlate best with SPEI-12. Agricultural land cover was considered as a factor, but there was no discernable trend associated with agricultural land use. BFI, length of record, size of watershed, location, or other

combinations of land cover also did not account for the differences.

Sign congruence does not address magnitude like correlation does, but it is a method to compare the overall patterns seen in SPEI data compared to flow data, as shown in Table 6. SDSF had slightly higher sign congruence than SDBF for SPEI-1. Sign congruence was comparable for SDBF and SDSF for SPEI-1 and SPEI-3, which suggests that flow separation for smaller time scales (1 - 3 months) is unnecessary and total flow is the practical variable to use in a standardized drought index. For longer time scales (12 months or greater) using baseflow appears to be a better variable in standardized drought indices.

5.2. Mann-Kendall

The watershed flow data (SDSF and SDBF) and SPEI data all have the same trend results. This finding is encouraging to consider SDBF, SDBF or other types of standardized flow data as regional proxy for drought indicators. The pattern seen in the northern watersheds of fluctuation wet/dry years corresponds to the precipitation patterns reported in WICCI (2021) [42]. From 1950-2020, the entire

Table 6. This table summarizes the results of the percentage of sign congruence between the SPEI time scales. The bold values represent the flow data (SDBF or SDSF) that had the highest sign congruence. For SPEI-1 and SPEI-3, SDSF has slightly higher sign congruence. For SPEI-12, SDBF has significantly higher sign congruence.

Watershed Name	*SPEI-1*		*SPEI-3*		*SPEI-12*	
	SDBF	**SDSF**	**SDBF**	**SDSF**	**SDBF**	**SDSF**
Allequash	70	67	70	67	70	67
Baraboo	66	67	69	70	72	67
Bear	80	83	80	83	80	83
Clinton	74	77	79	82	80	77
Fish	68	68	74	84	74	68
Fox	86	84	84	79	91	84
Grant	66	69	70	74	80	69
Kickapoo	63	64	69	70	73	64
Menomonee	75	78	80	80	75	78
Platte	67	68	70	71	71	68
Prairie	72	70	75	77	83	70
Pecatonica	74	70	74	72	77	70
Sparta	52	52	48	56	52	52
Spirit	76	76	84	84	86	76
White	64	64	64	62	81	64
Yahara	74	74	74	71	82	74
Yellow	68	70	75	75	75	70
Average	**70**	**71**	**73**	**73**	**76**	**71**

state's winters have been wetter. The southern part of the state has experienced the highest precipitation increases in all seasons, while the northern is a little wetter in spring and fall but drier in summer [42]. The northern summer dryness may dominate the increased wetness in the other seasons in certain areas. In other years, the other seasons' wetness dominates, which results in a wet/dry pattern that is observed in the SDBF, SDSF, and SPEI data for the northern watersheds.

5.3. Run Pattern

The run patterns for the flow (SDSF and SDBF) and SPEI (1, 3, and 12 months) data have similar patterns to one another, but these results show the difference between using baseflow data versus streamflow data in a drought index. The length of the SDBF positive and negative runs was longer than SDSF, and the run length occurred a little earlier. The max length of positive runs occurs later in the record and much earlier in the record for negative runs. This observation corresponds to WICCI (2021) [42] reports that the state is becoming wetter. It is significant to note that the positive run length occurred in 1993 and 1998 for SDBF and SDSF, which is much earlier than the SPEI. SPEI12 average positive run length was 2002, which comes the closest to the average values for the flows. It is expected that SPEI-12 will tend towards revealing long-term trends. Regardless, the differences indicate that standardized baseflow data may indicate wetness or possibly dry trends before SPEI-12.

Also of interest is that the positive run years for SPEI data are very similar to one another with the lowest variance among the run data. Negative run data have the highest variance and are comparable for both the SPEI and stream data. Some of this variance can be attributed to the wet and dry periods found in the northern part of the state. What is interesting is the similarities in the data despite SPEI data having a standard period (1901-2021), while the stream data end periods are different. The difference in these variances implies that the latter part of the record is substantially dominated by wetter conditions than have been seen across the state when either viewing streamflow data or model data derived from precipitation and ET.

5.4. Other Variables

It is unexpected to find little or no differences in the overall hydrologic patterns associated with land cover, watershed size, or baseflow index [43]. In particular, challenges persist in predicting flow in watersheds with recharge that changes seasonally and in large watersheds [44]. Agricultural watersheds with heavy summer irrigation were expected to have flow data that deviated from the SPEI flow data. These patterns may exist but at a seasonal scale that would be evident with monthly or seasonal data instead of annual.

6. Conclusions

Overall, some of the differences in SPEI and the SSI and SDBF are associated

with the development and nature of the data sets. SDSF and SDBF are taken from one watershed, while SPEI uses regional standardized precipitation. A regional-type SDBF may show very good agreement with unconfined aquifers and may provide a bridge between SPEI and groundwater data.

Standardized baseflow data shows good agreement with SPEI-12 and SPEI-3. Possibly with larger datasets with the same base period, agreement with SPEI-12 would be clearer. Standardized flow data shows better agreement with SPEI-3 and SPEI-1. Generally, two data types (flow and SPEI) show excellent pattern agreement. Annual mean standardized baseflow appears to be a better indicator of underlying and persisting patterns in watersheds with high baseflow contributions.

There is much work to be continued in the area of streamflow drought indices. The work in this paper demonstrates that baseflow data can be used to evaluate persistant drought patterns. For future work, drought analysis near the Great Lakes should incorporate stream data. Also, examining the seasonal flow patterns might be helpful in teasing out some groundwater anomalies associated with human pressures of irrigation.

Acknowledgements

The author would like to thank Chandra Page for proofreading drafts of this manuscript and anonymous reviewers whose suggestions improved this paper.

Conflicts of Interest

The author declares no conflicts of interest regarding the publication of this paper.

References

[1] Wilhite, D. and Glantz, M. (1985) Understanding: The Drought Phenomenon: The Role of Definitions. *Water International*, **10**, 111-120. https://doi.org/10.1080/02508068508686328

[2] Redmond, K. (2002) The Depiction of Drought: A Commentary. *Bulletin of the American Meteorological Society*, **83**, 1143-1147.

[3] Svoboda, M., Fuchs, B., World Meteorological Organization (WMO) and Global Water Partnership (GWP) (2016) Handbook of Drought Indicators and Indices. Integrated Drought Management Programme (IDMP), Integrated Drought Management Tools and Guidelines Series 2. https://public.wmo.int/en/resources/library/handbook-of-drought-indicators-and-indices

[4] Bachmair, S., Stahl, K., Collins, K., Hannaford, J., Acreman, M., Svoboda, M., Knutson, C., Smith, K., Wall, N., Fuchs, B., Crossman, N. and Overton I. (2016) Drought Indicators Revisted: The Need for a Wider Consideration of Environment and Society. *Wires Water*, **3**, 516-536. https://doi.org/10.1002/wat2.1154

[5] AghaKouchak, A., Mirchi, A., Madani, K., Baldassarre, G., Nazemi A., Alborzi, A., Anjileli, H., Azarderakhsh, M., Chiang, F., Hassanzadeh, E., Huning, L., Mallakpour, I., Martinez, A., Mazdiyasni, O., Moftakhari, H., Norouzi, H., Sadegh, M., Sa-

deqi, D., Van Loon, A. and Wanders, N. (2021) Anthropogenic Drought: Definition, Challenges, and Opportunities. *Reviews of Geophysics*, **59**, e2019RG000683. https://doi.org/10.1029/2019RG000683

[6] Trenberth, K., Dai, A., van der Schrier, G., Jones, P., Barichivich, J., Briffa, K. and Sheffield, J. (2013) Global Warming and Changes in Drought. *Nature Climate Change*, **4**, 17-22. https://doi.org/10.1038/nclimate2067

[7] Balti, H., Abbes, A., Mellouli, N., Farah, I., Sang, Y. and Lamolle, M. (2020) A Review of Drought Monitoring with Big Data: Issues, Methods, Challenges and Research Directions. *Ecological Informatics*, **60**, Article ID: 101136. https://doi.org/10.1016/j.ecoinf.2020.101136

[8] Lloyd-Hughes, B. (2013) The Impracticality of a Universal Drought Definition. *Theoretical and Applied Climatology*, **117**, 607-611. https://doi.org/10.1007/s00704-013-1025-7

[9] Hao, Z. and Singh, V. (2015) Drought Characterization from a Multivariate Perspective: A Review. *Journal of Hydrology*, **527**, 668-678. https://doi.org/10.1016/j.jhydrol.2015.05.031

[10] Crausbay, S., Ramirez, A., Carter, S., Cross, M., Hall, K., Bathke, D., Betancourt, J., Colt, S., Cravens, A., Dalton, M., Dunham, J., Hay, L., Hayes, M., McEvoy, J., McNutt, C., Moritz, M., Nislow, K., Raheem, N. and Sanford, T. (2017) Defining Ecological Drought for the Twenty-First Century. *Bulletin of the American Meteorological Society*, **98**, 2543-2550. https://doi.org/10.1175/BAMS-D-16-0292.1

[11] Barlow, P., Cunningham, W., Zhai, T. and Gray, M. (2015) U.S. Geological Survey Groundwater Toolbox, a Graphical and Mapping Interface for Analysis of Hydrologic Data (Version 1.0): User Guide for Estimation of Base Flow, Runoff, and Groundwater Recharge from Streamflow Data. U.S. Geological Survey Techniques and Methods. https://doi.org/10.3133/tm3B10

[12] USGS (US Geological Survey) (2023) Web Interface: U.S. Geological Survey National Water Information System Web Site. http://waterdata.usgs.gov/nwis/

[13] McKee, T.B., Doesken, N.J. and Kleist, J. (1993) The Relationship of Drought Frequency and Duration to Time Scales. 8*th Conference on Applied Climatology*, Anaheim, 17-22 January 1993, 179-184.

[14] Vicente-Serrano S., Beguería S. and López-Moreno, J. (2010) A Multi-Scalar Drought Index Sensitive to Global Warming: The Standardized Precipitation Evapotranspiration Index. *Journal of Climate*, **23**, 1696-1718. http://digital.csic.es/handle/10261/22405 https://doi.org/10.1175/2009JCLI2909.1

[15] Vicente-Serrano, S.M., Beguería, S., López-Moreno, J., Angulo, M. and Kenawy, E. (2010) A New Global 0.5° Gridded Dataset (1901-2006) of a Multiscalar Drought Index: Comparison with Current Drought Index Datasets Based on the Palmer Drought Severity Index. *Journal of Hydrometeorology*, **11**, 1033-1043. http://digital.csic.es/handle/10261/23906 https://doi.org/10.1175/2010JHM1224.1

[16] Beguería, S., Vicente-Serrano, S., Reig, F. and Latorre, B. (2014) Standardized Precipitation Evapotranspiration Index (SPEI) Revisited: Parameter Fitting, Evapotranspiration Models, Tools, Datasets and Drought Monitoring. *International Journal of Climatology*, **34**, 3001-3023. https://doi.org/10.1002/joc.3887

[17] Vicente-Serrano, S.M. and National Center for Atmospheric Research Staff (2022) The Climate Data Guide: Standardized Precipitation Evapotranspiration Index (SPEI). https://climatedataguide.ucar.edu/climate-data/standardized-precipitation-evapotra

nspiration-index-spei

[18] Guttman, N. (2007) Accepting the Standardized Precipitation Index: A Calculation Algorithm. *JAWRA Journal of the American Water Resources Association*, **35**, 311-322. https://doi.org/10.1111/j.1752-1688.1999.tb03592.x

[19] Vicente-Serrano, S., López-Moreno, J., Beguería, S., Lorenzo-Lacruz, J., Azorin-Molina, C. and Moran_Tejeda, E. (2012) Accurate Computation of a Streamflow Drought. *Journal of Hydraulic Engineering*, **17**, 318-332. https://doi.org/10.1061/(ASCE)HE.1943-5584.0000433

[20] Kraft, G.J., Clancy, K., Mechenich, D.J. and Haucke, J. (2012) Irrigation Effects in the Northern Lake States: Wisconsin Central Sands Revisited. *Ground Water*, **50**, 308-318. https://doi.org/10.1111/j.1745-6584.2011.00836.x

[21] Sloto, R.A. and Crouse, M.Y. (1996) HYSEP—A Computer Program for Streamflow Hydrograph Separation and Analysis: U.S. Geological Survey Water-Resources Investigations Report 96-4040. http://pubs.er.usgs.gov/publication/wri964040

[22] Klaus, J. and McDonnell, J. (2013) Hydrograph Separation Using Stable Isotopes: Review and Evaluation. *Journal of Hydrology*, **505**, 47-64. https://doi.org/10.1016/j.jhydrol.2013.09.006

[23] Pelletier, A. and Andréassian, V. (2020) Hydrograph Separation: An Impartial Parametrisation for an Imperfect Method. *Hydrology and Earth System Sciences*, **24**, 1171-1187. https://doi.org/10.5194/hess-24-1171-2020

[24] Eckhardt, K. (2023) How Physically Based Is Hydrograph Separation by Recursive Digital Filtering? *Hydrology and Earth System Sciences*, **27**, 495-499. https://doi.org/10.5194/hess-27-495-2023

[25] Penna, D. and van Meerveld, H. (2019) Spatial Variability in the Isotopic Composition of Water in Small Catchments and Its Effect on Hydrograph Separation. *Wires Water*, **6**, e1367. https://doi.org/10.1002/wat2.1367

[26] Shao, G., Zhang, D., Guan, Y., Sadat, M.A. and Huang, F. (2020) Application of Different Separation Methods to Investigate the Baseflow Characteristics of a Semi-Arid Sandy Area, Northwestern China. *Water*, **12**, Article 434. https://doi.org/10.3390/w12020434

[27] Markovich, K., Dahlke, H., Arumí, J., Maxwell, R. and Fogg, G. (2019) Bayesian Hydrograph Separation in a Minimally Gauged Alpine Volcanic Watershed in Central Chile. *Journal of Hydrology*, **575**, 1288-1300. https://doi.org/10.1016/j.jhydrol.2019.06.014

[28] Shilling, K., Langel, R., Wolter, C. and Areas-Amado, A. (2021) Using Baseflow to Quantify Diffuse Groundwater Recharge and Drought at a Regional Scale. *Journal of Hydrology*, **602**, Article ID: 126765. https://doi.org/10.1016/j.jhydrol.2021.126765

[29] Troolin, W. and Clancy, K. (2016) Comparison of Three Delineation Methods Using the Curve Number Method to Model Runoff. *Journal of Water Resource and Protection*, **8**, 945-964. https://doi.org/10.4236/jwarp.2016.811077

[30] Jenson, S. (1984) Automated Derivation of Hydrological Basin Characteristics from Digital Elevation Data. US Geological Survey Report 14-08-0001-20129. http://topotools.cr.usgs.gov/pdfs/automated-derivation-of-hydrologic-basin-characteristics-from-digital-elevatioin-model-data.pdf

[31] USGS (US Geological Survey) (2019) NED (National Elevation Data) 2020 Elevation. SDE Raster Digital Data. http://nationalmap.gov/elevation.html

[32] USGS (US Geological Survey) (2020) NLCD (National Land Cover Database) 2020

Land Cover. SDE Raster Digital Data. https://www.mrlc.gov/

[33] Mann, H.B. (1945) Nonparametric Tests against Trend. *Econometrica*, **13**, 245-259. https://doi.org/10.2307/1907187

[34] Kendall, M.G. (1975) Rank Correlation Methods. Oxford University Press, New York.

[35] Helsel, D. and Hirsch, R. (1992) Statistical Methods in Water Resources. Elsevier, Amsterdam.

[36] Milly, P., Betancourt, J., Falkenmark, M., Hirsch, R., Kundzewicz, Z., Lettenmaier, D. and Stouffer, R. (2008) Stationarity Is Dead: Whither Water Management? *Science*, **319**, 573-574. https://doi.org/10.1126/science.1151915

[37] Milly, P., Betancourt, J., Falkenmark, M., Hirsch, R., Kundzewicz, Z., Lettenmaier, D. and Stouffer, R. (2015) On Critiques of "Stationarity Is Dead: Whither Water Management?" *Water Resource Research*, **51**, 7785-7789. https://doi.org/10.1002/2015WR017408

[38] Wang, F., Shao, W., Yu, H., Kan, G., He, X., Zhang, D., Ren, M. and Wang, G. (2020) Re-Evaluation of the Power of the Mann-Kendall Test for Detecting Monotonic Trends in Hydrometeorological Time Series. *Frontiers in Earth Science*, **8**, Article 494616. https://doi.org/10.3389/feart.2020.00014

[39] Moye, L. and Kapadia, A. (1995) Predictions of Drought Length Extreme Order Statistics Using Run Theory. *Journal of Hydrology*, **169**, 95-110. https://doi.org/10.1016/0022-1694(94)02662-U

[40] Smakhtin, V.U. (2001) Low Flow Hydrology: A Review. *Journal of Hydrology*, **240**, 147-186. https://doi.org/10.1016/S0022-1694(00)00340-1

[41] Heinrich, G. and Andreas, G. (2011) The Future of Dry and Wet Spells in Europe: A Comprehensive Study Based on the ENSEMBLES Regional Climate Models. *International Journal of Climatology*, **32**, 1951-1970. https://doi.org/10.1002/joc.2421

[42] Wisconsin Initiative on Climate Change Impacts (WICCI) (2021) Wisconsin's Changing Climate: Impacts and Solutions for a Warmer Climate. 2021 Assessment Report: Wisconsin's Changing Climate, Nelson Institute for Environmental Studies, University of Wisconsin-Madison and the Wisconsin Department of Natural Resources, Madison, WI.

[43] Briggs, M., Gazoorian, C., Doctor, D. and Burns, D. (2022) A Multiscale Approach for Monitoring Groundwater Discharge to Headwater Streams by the U.S. Geological Survey Next Generation Water Observing System Program—An Example from the Neversink Reservoir Watershed, New York. U.S. Geological Survey Fact Sheet 2022-3077. https://doi.org/10.3133/fs20223077

[44] Clancy, K. (2021) Evaluating the Effect of Land Cover, Seasonality and Delineation Method on Runoff at the Watershed Scale. *Journal of Water Resource and Protection*, **13**, 750-765. https://doi.org/10.4236/jwarp.2021.139039